Neutron scattering studies of nucleosome structure at low ionic strength

Edward C. Uberbacher, Venkatraman Ramakrishnan, Donald E. Olins, and Gerard J. Bunick

Biochemistry, **1983**, 22 (21), 4916-4923• DOI: 10.1021/bi00290a007 • Publication Date (Web): 01 May 2002

Neutron Scattering Studies of Nucleosome Structure at Low Ionic Strength†

Edward C. Uberbacher, Venkatraman Ramakrishnan,‡ Donald E. Olins, and Gerard J. Bunick*

ABSTRACT: Ionic strength studies using homogeneous preparations of chicken erythrocyte nucleosomes containing either 146 or 175 base pairs of DNA show a single unfolding transition at about 1.5 mM ionic strength as determined by small-angle neutron scattering. The transition seen by some investigators at between 2.9 and 7.5 mM ionic strength is not observed by small-angle neutron scattering in either type of nucleosome particle. The two contrasts measured (H_2O and D_2O) indicate that only small conformational changes occur in the protein core, but the DNA is partially unfolded below the transition point. Patterson inversion of the data and analysis of models indicate that the DNA in both types of particle is unwinding from the ends, leaving about one turn of supercoiled DNA bound to the histone core in approximately its normal (compact) conformation. The mechanism of unfolding appears to be similar for both types of particles and in both cases occurs at the same ionic strength. The unfolding observed for nucleosomes in this study is in definite disagreement with extended superhelical models for the DNA and also disagrees with models incorporating an unfolded histone core.

The structural and dynamical properties of nucleosomes are a current subject of intense investigation. Changes in DNA accessibility in transcriptionally active genes suggest that structural alterations affect the functional state of specific segments of the genome (Weintraub &Groudine, 1976). It is likely that important events such as transcription and replication are regulated, at least in part, by local changes in chromatin structure on the level of the nucleosome.

One way to characterize the ability of nucleosomes to unfold has been to examine their response to variations in ionic strength. Reduced ionic strength causes a reversible unfolding of nucleosome core particles without loss of proteins. This low-salt transition has been studied by a wide variety of methods including hydrodynamics (Gordon et al., 1978, 1979; Harrington, 1981), fluorescence measurements (Dieterich et al., 1979; Eshaghpour et al., 1980; Libertini & Small, 1982), electron microscopy (Oudet et al., 1977), electrooptical techniques (Crothers et al., 1978; Wu et al., 1979; Schlessinger et al., 1982), and chemical cross-linking (Martinson et al., 1979). A consensus has emerged that one relatively complex transition occurs centered at about 1.5 mM ionic strength in core particles with 146 base pair (bp)[1] DNA and also in particles with longer length DNA (Schlessinger et al., 1982). A second transition at between 3 and 7 mM ionic strength has been observed by some investigators in particles consisting of about 140 base pairs (Gordon et al., 1978) and in particles with 175 base pair DNA (Schlessinger et al., 1982).

Despite the extensive investigation of these transitions, there seems to be little agreement as to the mode or mechanism of unfolding, the degree of unfolding, the flexibility or rigidity of the unfolded structure, and the extent to which the histones are involved in the process. Evidence from fluorescence (Dieterich et al., 1979; Eshaghpour et al., 1980) and UV cross-linking data (Martinson et al., 1979) indicates that some conformational change in the histones is most likely required, but the extent of this change is still in question. The conformation of the DNA below the transition(s) is also uncertain. Currently proposed models range from extended superhelical forms with lengths of about 500 Å and axial ratios of about 10:1 [for 146 base pair particles (Harrington, 1981) and 175 base pair particles (Schlessinger et al., 1982)] to oblate ellipsoids with axial ratios near 3:1 (Wu et al., 1979). To add to this uncertainty, the results obtained at low ionic strength seem to be dependent upon the type and condition of the nucleosomes used, the range of DNA lengths present, and the particular experimental method used to follow the transition(s).

In the present study, small-angle neutron scattering has been used to examine the conformation of very homogeneous preparations of 146 and 175 base pair nucleosomes as a function of ionic strength ranging from 15 mM total ionic strength to 0.46 mM total ionic strength. The use of contrast variation in small-angle neutron scattering provides a direct method of evaluating models for histone and DNA conformations at the appropriate ionic strength conditions. The low concentration of nucleosomes used in this experiment (as low as 0.35 mg/mL) allows direct comparison of the results obtained here with electrooptical and hydrodynamic data. Furthermore, the purity and homogeneity of the preparations of 146 and 175 base pair nucleosomes used here are significantly better than in previous studies. This study should serve to provide suitable physical parameters for the low ionic strength transitions in nucleosomes.

Materials and Methods

Preparation of Nucleosomes. Chicken erythrocyte nuclei were isolated from 300 mL of blood by the method of Hewish & Burgoyne (1973). Half of the nuclear pellet was treated to yield mostly 175 bp nucleosomes by using a modification of Crothers' method (Crothers et al., 1978) as follows: Di-

† From the University of Tennessee—Oak Ridge Graduate School of Biomedical Sciences and Biology Division (E.C.U., D.E.O., and G.J.B.), and the National Center for Small Angle Scattering Research (V.R.), Oak Ridge National Laboratory, Oak Ridge, Tennessee 37830. *Received March 11, 1983.* Supported by Grants GM 29818 (to G.J.B.) and GM 19334 (to D.E.O.) from the National Institutes of Health, by the National Science Foundation under Grant DMR-77-24458 with the U.S. Department of Energy, and by the Office of Health and Environmental Research, U.S. Department of Energy, under Contract W-7045-eng-26 with the Union Carbide Corp.

‡ Present address: Biology Department, Brookhaven National Laboratories, Upton, NY 11973.

[1] Abbreviations: bp, base pair(s); TE buffer, 10 mM Tris and 1.0 mM EDTA, pH 7.0; EDTA, (ethylenedinitrilo)tetraacetic acid (disodium salt); Tris, tris(hydroxymethyl)aminomethane; Tes, *N*-[tris(hydroxymethyl)methyl]-2-aminoethanesulfonic acid; PMSF, phenylmethanesulfonyl fluoride (50 mM stock in 2-propanol); H1, H5, H2A, H2B, H3, and H4, the respective histones; HMG 14/17, the respective high mobility group proteins; Pipes, piperazine-*N*,*N*′-bis(2-ethanesulfonic acid).

0006-2960/83/0422-4916$01.50/0

gestion time for the nuclei was determined by a small-scale test digestion in which 1.0 mL of nuclei, A_{260} = 100 (read in 0.1 N NaOH), was digested at 30 °C with 497 units of micrococcal nuclease and 1 mM $CaCl_2$. At specified time points, 45-μL aliquots were removed to vials containing 5 μL of 50 mM EDTA to stop the reaction. Samples were electrophoresed on an 8% polyacrylamide single-strand gel as described by Lutter (1978). The optimum digestion time for the preparation of 175 bp nucleosomes was determined by visual inspection of the stained gel.

The bulk of the nuclei (75.6 mL, A_{260} = 100, 1 mM $CaCl_2$) were digested with 497 units of micrococcal nuclease per mL at 37 °C for 30 min. The reaction was stopped by making the solution 1 mM in EDTA, followed by chilling to 4 °C. The nuclei were centrifuged for 2 min at 8000*g*. The nuclear pellet was resuspended in 0.2 mM EDTA, pH 7.0. Lysis of the nuclei was accomplished by repeated pipetting of the suspension. After centrifugation, about half of the soluble chromatin fraction (1850 A_{260} units) was loaded onto a 6 × 200 cm Sephacryl S-300 column equilibrated in 5 mM EDTA and 10 mM Tris, pH 7.6. The yield of 175 bp nucleosomes was approximately 88 mg. These particles contained the unproteolyzed histone octamer and were completely free of histones H1 and H5.

Nucleosomes containing 146 bp DNA were isolated by a modified version of the procedure described by Lutter (1978). Changes to the procedure were made as follows: A 6 × 200 cm Sephacryl S-300 column equilibrated with 20 mM NaCl–5 mM Tris-HCl, pH 7.5, 0.2 mM EDTA, and 2 mM β-mercaptoethanol was used to isolate the monomer nucleosomes after digestion. Pooled monomer fractions were then dialyzed against 100 mM KCl, 12 mM $MgCl_2$, and 1 mM Pipes, pH 7.2, at 4 °C. After dialysis, any insoluble material present was removed by centrifugation at 8000*g* for 20 min. The supernatant was dialyzed against 5 mM Tes, pH 7.4, 20 mM NaCl, and 0.2 mM EDTA. Nucleosomes were concentrated to 10–20 mg/mL and stored at 4 °C. Throughout the isolation, solutions were made 0.1 mM in PMSF and 3.0 mM in NaN_3 to inactivate serine proteases and inhibit bacterial growth.

The nucleosomes obtained by this procedure are highly homogeneous, containing 146 ± 2 bp of DNA and a full complement of unproteolyzed core histones. For the neutron scattering study, both the 175 and 146 bp nucleosomes were further purified by preparative polyacrylamide gel electrophoresis using a modified Buchler Poly-Prep 200 (E. C. Uberbacher and G. J. Bunick, unpublished results). Figure 1 shows single-stranded DNA and particle gels for the 146 and 175 bp nucleosomes.

Sample Preparation. Samples of 146 and 175 bp nucleosomes were prepared by dialysis against three 12-h changes of appropriate dilutions of 2 × TE buffer. Appropriate concentrations of TE buffer needed in the dialysate to reach a desired ionic strength with a given nucleosome concentration in the sample were calculated by using the Donnan equilibrium method. This method takes into account the fact that counterions associated with charged macromolecules affect the equilibrium. With assumptions of electrical neutrality and equal activities of diffusible components across the membrane, the following formula relates the relevant parameters:

$$I_D^2 = (I_S - I_N)I_S$$

where I_D is the dialysate ionic strength, I_N is the ionic strength contribution from 146 or 175 bp nucleosomes (with counterions) at the nucleosome concentration of the sample, and I_S is the ionic strength of the sample. The ionic strength contribution of 146 bp nucleosomes was calculated by assuming 200 mobile counterions (Libertini & Small, 1982) and 258 mobile counterions for 175 bp nucleosomes. The ionic strength contribution from buffer components was calculated for pH 7.0 by assuming Tris was 95% dissociated and Na_2EDTA fully dissociated. Changes in nucleosome concentration during dialysis were taken into account in the calculation of ionic strength of the samples. Concentrations were calculated from the A_{260} absorbance measured on a Cary 14 scanning spectrophotometer before and after neutron scattering.

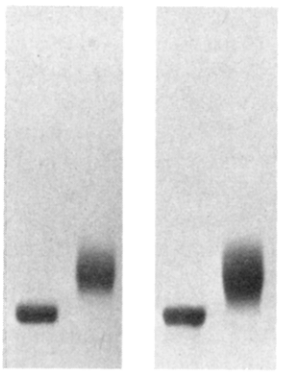

FIGURE 1: Five percent polyacrylamide particle and single-strand DNA gels showing the 146 and 175 bp nucleosomes used in this study. (A) Single-strand DNA gel of 146 bp nucleosomes; (B) single-strand DNA gel of 175 bp nucleosomes; (C) particle gel of 146 bp nucleosomes; (D) particle gel of 175 bp nucleosomes.

Neutron Scattering Methods. D_2O (99%) was redistilled prior to its use in scattering buffers. All buffers were adjusted to an apparent pH of 7.0. The final D_2O concentrations in the samples and buffers were determined by neutron transmission measurements. Scattering and transmission measurements were done in either 1.0- or 5.0-mm path-length cylindrical quartz cells. Sample and buffer were run in the same cell or in a pair of matched cells to avoid systematic errors due to slight differences in cell thickness or cell transmission. In general, the transmissions of sample and buffer were the same within error. In those few cases where the transmissions were slightly different, the composition of the buffer was adjusted by the addition of the appropriate amount of H_2O or D_2O to make the transmissions equal.

Neutron measurements were done on the 30-m small-angle neutron scattering instrument of the National Center for Small Angle Scattering Research at Oak Ridge National Laboratory. The instrument selects neutrons of λ = 4.75 Å with a $\Delta\lambda/\lambda$ of 6%. To optimize flux, the largest combination of slit sizes (3.5 cm in diameter at source, 1.74 cm at sample) was chosen that would still allow us to detect large radii of gyration [corresponding to a K of 0.007 A^{-1}, where $K = (4\pi/\lambda)\sin\theta$]. Since the signal to noise ratio in D_2O is substantially higher than that in H_2O (due to the large incoherent background from hydrogen scattering), counting times are much shorter in D_2O than in H_2O. Furthermore, the high transmission of D_2O (~0.93 for 1-mm path length) makes it possible to use longer path lengths (5 mm). The scattered neutrons are detected by a two-dimensional position-sensitive ^3He detector with 64 × 64 1-cm^2 elements. The sample detector distance is variable from 1.5 to 20 m. The data were collected at room temperature (23 °C).

In the present study, the range of contrast accessible is limited to measurements in H_2O and D_2O which represent the two highest contrasts available. This is due to the fact that quite low concentrations (0.35 mg/mL) of nucleosomes have to be used in order to avoid problems from the Donnan effect.

Since DNA and protein have quite different relative contrasts in H_2O and D_2O, measurements at these two contrasts provide a basis for separating the contributions of DNA and protein.

Since the signal to noise ratio is so low for the lower ionic strength samples (concentrations sometimes smaller than 0.5 mg/mL), considerable care was taken to avoid systematic errors. Repeated measurements were made on the sample and buffer by cycling them manually every few hours. The various H_2O buffer runs, which also serve to calibrate the detector sensitivity and calculate the scattering on an absolute scale, showed virtually no difference from one run to the next, indicating that the stability of the instrument was excellent and was not a source of systematic errors.

Analysis of Neutron Data. The method of contrast variation is well documented in the literature (Engelman & Moore, 1975; Hjelm et al., 1977; Braddock et al., 1981; Stuhrmann & Duee, 1975). The use of two or more different contrasts (corresponding to different H_2O/D_2O ratios in the buffers) constrains models much more than a single experiment, since the relative contributions of DNA and protein are different in H_2O and D_2O. Calculation of proton exchange in the different solvents was done according to Hjelm et al. (1977).

The raw data are present in the form of a 64 × 64 array. The data were normalized to 1000 monitor counts and to unit thickness and transmission and were corrected for background and detector sensitivity prior to radial averaging. The radially averaged curves of intensity [$I(k)$] as a function of $k = (4\pi/\lambda) \sin \theta$ were stored for further analysis. Statistical errors were propagated throughout the analysis and are reflected in the final estimates of parameters.

(*i*) *Guinier Analysis.* In the low k region, small-angle scattering data obey Guinier's law: $I(k) = I(0)e^{-k^2R_g^2/3}$, where $I(0)$ is the forward scatter and R_g is the radius of gyration. Both $I(0)$ and R_g were determined by a weighted least-squares fit to a plot of ln $I(k)$ vs. k^2.

(*ii*) $P(r)$ *Analysis.* Much information can be obtained from $P(r)$ which is called the length distribution function or radial Patterson function, defined by

$$P(r) = \frac{2r}{\pi}\int_0^\infty kI(k) \sin (kr)\, dk$$

$P(r)$ is the distribution of point to point distances (weighted by the scattering lengths) within the particle. The evaluation of $P(r)$ cannot be done directly since the data are not complete: $I(k)$ is missing at very low angles due to the presence of the beam stop, and high-angle data are missing due to a finite detector size and a low signal to noise ratio in the measurable high k region. $P(r)$ was evaluated by using the indirect Fourier transformation algorithm of Moore (1980). With the normalization factor chosen above for $P(r)$, one can also evaluate $I(0)$ and R_g:

$$I(0) = \int_0^\infty P(r)\, dr$$

and

$$R_g = \left[\tfrac{1}{2}\int_0^\infty r^2P(r)\, dr\right] \Big/ \left[\int_0^\infty P(r)\, dr\right]$$

Thus, $I(0)$ and R_g can be evaluated by a method which uses the entire scattering curve rather than the Guinier region alone.

A comparison of calculated $P(r)$ functions for models with the observed $P(r)$ offers a much more detailed test than a comparison of radii of gyration alone. It is also intuitively very useful since $P(r)$ correlates directly to size, shape, and density distribution of a particle.

For modeling purposes, the histone core in all cases was represented by a cylinder of uniform density with a diameter of 90 Å and a thickness of 42 Å. These parameters are generally consistent with previous neutron scattering models of nucleosomes (Braddock et al., 1981) and fit experimentally determined protein R_g's. The DNA for "compact" nucleosomes was modeled as a 1.7-turn superhelix with a radius of 48 Å and a pitch of 30 Å. The DNA helix itself was assumed to have a diameter of 20 Å. The models proposed later in this study for 146 and 175 bp nucleosomes at low ionic strength are based upon the compact nucleosome except that the DNA tail regions (DNA not in the innermost superhelical turn) no longer follow a superhelical path but are represented by two straight cylinders of appropriate length and 20-Å diameter extending in opposite directions (see Figure 7). For the "extended form" of the nucleosome (Schlessinger et al., 1982), the DNA was assumed to extend along the superhelical axis in a superhelical path with 2.0 turns, giving rise to a maximum dimension of 470 Å and an outside diameter of 65 Å. The histone core was modeled as in the compact particle since this gave the best fit to the data.

Sedimentation Methods. Sedimentation studies were carried out on a Beckman Model E analytical ultracentrifuge, equipped with UV optics, a photoelectric scanner, and a multiplexer. Double-sector cells were used for the study. The output of the photomultiplier was interfaced to a PDP 11/40 computer. All runs were done at 21.3 °C with a rotor speed of 30 000 rpm. Scans were collected at intervals of 16 min.

The digitized scan data were differentiated, and the positions of the second moment (r_B) of the gradient curve were calculated as a function of time.

Plots of ln r_B vs. time were linear, and the slope of the lines determined by a least-squares fit yielded the sedimentation coefficients. Coefficients were corrected for viscosity, buoyancy, and temperature effects to yield $s_{20,w}$ values, the effective sedimentation coefficients in water at 20 °C.

Concentrations of the samples were determined by measuring the A_{260} with a Cary 14 spectrophotometer.

Results

Characterization of the 175 bp Nucleosome at High Ionic Strength. The radius of gyration and the forward scatter were measured for the 175 bp nucleosome at high ionic strength (60 mM) in H_2O, 24.5% D_2O, 74.5% D_2O, and 96% D_2O. From a plot of $[I(0)]^{1/2}$ vs. percent D_2O, the contrast match point (where the forward scatter vanishes) was determined. The observed value of 49.4 ± 0.4% D_2O is in good agreement with the value of 50.1% D_2O calculated from the scattering density. A plot of R_g^2 vs. the inverse contrast ($1/\bar{\rho}$) was fit with a straight line in order to obtain α, which describes the change in scattering length density as one moves out from the center of the particle. The value of α obtained is basically consistent with the normal compact conformation of the nucleosome (DNA outside and protein core inside). β for the 175 bp nucleosome was small and could not be measured within the accuracy of the experiment, indicating that the centers of mass of the DNA and protein are approximately coincident.

The experimentally determined length distribution function [$P(r)$] for the particle at 15 mM ionic strength is, as expected, consistent with that of a compact nucleosome (see Figure 6). Therefore, a detailed modeling analysis was not considered. The slightly higher R_g for the DNA in this particle compared to a 146 bp nucleosome implies that some portion or all of the DNA may be at a slightly higher radius than in the 146 bp particle. A large body of evidence suggests that the DNA tails in the 175 bp nucleosome are very loosely bound to the core (Lutter, 1978), so a likely possibility is that these tails represent the portion of DNA at higher radius. A summary of param-

Table I: Characteristics for the 175 bp Particle in the Compact State

radii of gyration (Å)	
at infinite contrast	43.2 ± 0.5
protein-dominated	34.1 ± 1.5
DNA-dominated	52.1 ± 1.3
density at match point (cm^{-2})	
obsd value	2.88×10^{10}
calcd value	2.93×10^{10}
particle volume ($Å^3$)	
obsd value	2.42×10^5
calcd value	2.39×10^5
α	$(6.0 \pm 0.9) \times 10^{-4}$

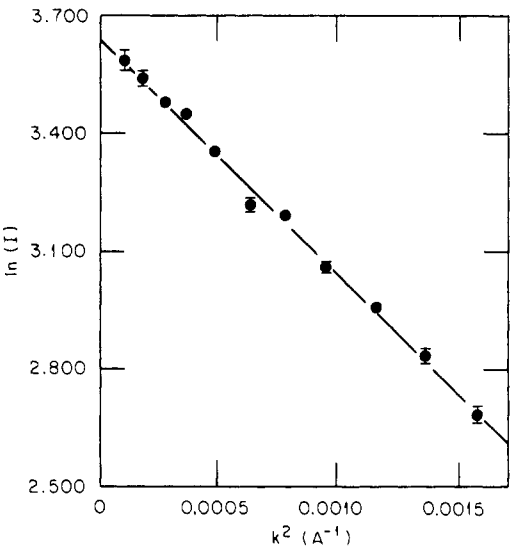

FIGURE 2: Guinier plot of 175 bp nucleosomes at 3 mM total ionic strength in D_2O buffer (above the transition point for unfolding). The radius of gyration (42.5 Å) indicates a compact particle.

eters calculated for the 175 bp nucleosome at 15 mM ionic strength is shown in Table I.

Changes of 175 and 146 bp Nucleosomes with Ionic Strength. Both kinds of nucleosomes were studied in D_2O at six different ionic strengths ranging from 0.46 to 15 mM. The final ionic strength of each sample was calculated from the actual concentration of nucleosomes in the sample and the known ionic strength of the dialysate buffer. Conductivity measurements of the lowest ionic strength samples were made and compared to KCl and TE standards between 0.01 and 10 mM ionic strength in order to ensure that no errors in the calculation of ionic strength had occurred. The agreement between calculated and measured ionic strengths was excellent, indicating we had obtained the low ionic strengths desired (~0.5 mM). There was also some concern that excess divalent ions sequestered by the nucleosome might inhibit unfolding since the concentration of EDTA in the lowest ionic strength buffer was low. To eliminate this possibility, flameless and flame atomic absorption spectroscopy studies were done on aliquots from the lowest ionic strength samples. The analysis showed that the concentration of divalent ions bound to nucleosomes was 5.7 μM, with 0.4 μM divalent ions free in the buffer solution. This amounts to about 4.5 divalent ions bound to each nucleosome, which is extremely minimal. According to dichroism data (Wu et al., 1979), an order of magnitude higher concentration of divalent ions is necessary to begin to inhibit unfolding.

A concentration series was done for nucleosomes at the highest ionic strength (~15 mM). The ratio $I(k)/c$ (where c is nucleosome concentration) calculated from the scattering

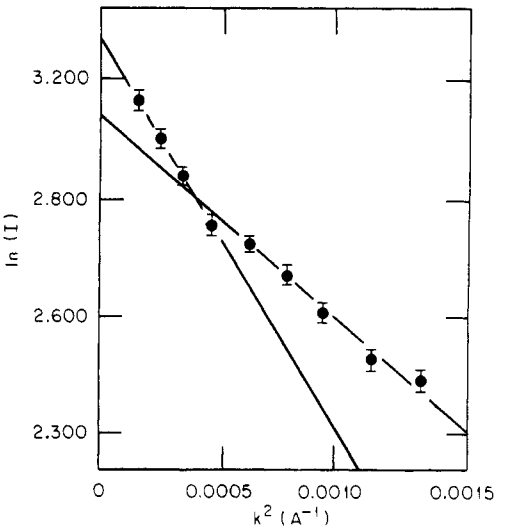

FIGURE 3: Guinier plot of 175 bp nucleosomes at 1.35 mM total ionic strength in D_2O buffer (below the transition point for unfolding). The radius of gyration (55.5 Å) in the true Guinier region (k^2 up to 0.0006 $Å^{-1}$) indicates an unfolded particle. The break in the Guinier plot at $k^2 = 0.0006$ $Å^{-1}$ indicates the particle has a compact center and also has extended regions which are less dense.

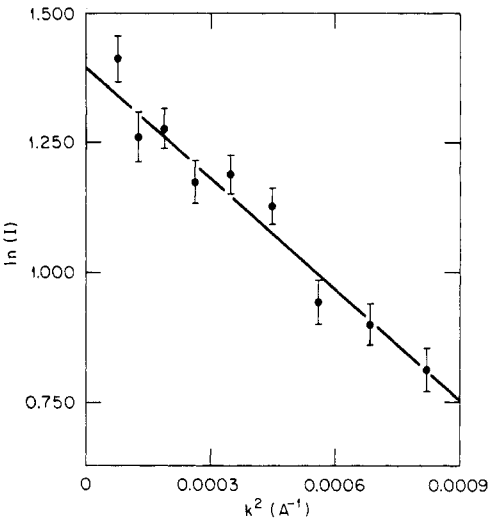

FIGURE 4: Data from the true Guinier region for 146 bp nucleosomes at 0.5 mM ionic strength in D_2O buffer (below the transition point for unfolding) collected at 7.5 m. These data demonstrate that the true Guinier region is linear and has a well-defined shape.

curves showed little change, indicating that no significant aggregation or interparticle effects occurred over the range studied.

Neutron scattering measurements were initially done for all samples at a 3.2-m sample to detector distance (observable k range of 0.012–0.17 $Å^{-1}$). Above 2 mM ionic strength, Guinier plots were linear to the first observable point outside the beam stop (Figure 2). Below 2 mM ionic strength, the first few observable points showed a marked departure in slope from the rest of the curve (Figure 3). This kind of "broken" Guinier plot is characteristic of a particle with a compact core and an extended shell region (Kratky, 1963).

Samples above and below 2 mM ionic strength were remeasured by using a sample to detector distance of 7.5 m (k from 0.007 to 0.07 $Å^{-1}$). The scattering curves gave Guinier plots with the same radii of gyration as obtained from the innermost points of the 3.2-m data (Figure 4). To rule out the possibility that the increase in R_g at low ionic strength was due to aggregation, values of $I(0)/c$ were evaluated by careful

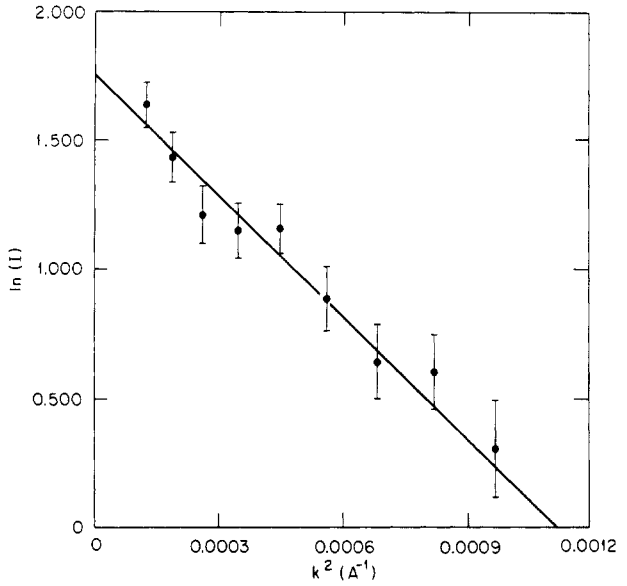

FIGURE 5: Data from the true Guinier region for 175 bp nucleosomes at 1.35 mM ionic strength in H_2O buffer (below the transition for unfolding) collected at 7.5 m.

Table II: Values for Radii of Gyration as a Function of Ionic Strength

buffer	ionic strength (mM)	measured nucleosome concn (mg/mL)	radius of gyration (Å)
		146 bp Particle	
D_2O	14.9	1.78	37.6 ± 1.0
	6.9	1.78	36.8 ± 0.4
	2.8	0.73	38.3 ± 0.7
	2.0	0.84	46.4 ± 2.9
	1.3	0.44	43.4 ± 4.1
	0.5	0.38	47.0 ± 3.0
		175 bp Particle	
D_2O	14.8	1.76	41.5 ± 0.5
	6.7	1.52	42.6 ± 0.6
	2.9	0.80	42.5 ± 1.5
	2.0	0.79	42.0 ± 1.0
	1.3	0.50	55.5 ± 2.0
	0.5	0.44	56.8 ± 2.0
H_2O	15.0	2.31	45.2 ± 1.3
	0.5	0.35	67.0 ± 7.0

measurements of sample concentration. This ratio did not change significantly. $I(0)/c$ was also examined on an absolute scale, by comparison with the incoherent scatter of water (Jacrot & Zaccai, 1981). Calculated values agreed with observed values, showing the absence of significant amounts of aggregation.

Both kinds of nucleosomes were studied in H_2O at the extremes of ionic strength (0.46 and 15 mM). These required very long run times. A Guinier plot of the 175 bp nucleosome at low ionic strength in H_2O is shown in Figure 5. For the 146 bp nucleosome in low ionic strength H_2O buffer, insufficient time was available to achieve sufficiently good statistics. The changes in the radius of gyration with ionic strength are shown in Table II.

With a Beckman Model E analytical ultracentrifuge, values for the sedimentation coefficients were also determined for 175 and 146 bp nucleosomes in low and high ionic strengths. These were typically done by using very low concentrations of nucleosomes (~0.05 mg/mL). In addition, one of the low ionic strength samples in D_2O was measured at its concentration during scattering (0.45 mg/mL). The sedimentation scans showed no apparent sign of aggregation, and further, the value of $s_{20,w}$ obtained from the more concentrated low ionic strength sample was the same as that obtained from the more dilute sample. This indicates that concentration effects were negligible. The primary charge effect for nucleosomes under these conditions has been shown to be negligible by Gordon et al. (1979), who found no change in $s_{20,w}$ with ionic strength for cross-linked nucleosomes.

Table III: Sedimentation Coefficients under Various Conditions for 175 and 146 bp Nucleosomes

sample	concn (mM)	buffer	$s_{20,w}$ (S)
146 bp	0.086	15 mM TE	11.4
146 bp	0.086	0.5 mM TE	10.5
175 bp	0.080	15 mM TE	11.7
175 bp	0.080	15 mM TE, D_2O	12.1
175 bp	0.080	0.5 mM TE	10.5
175 bp	0.44	0.6 mM TE, D_2O	10.4

The values of the sedimentation coefficient are shown in Table III. The values at higher ionic strength agree well with previously measured values (Gordon et al., 1979). The smaller $s_{20,w}$ values from low ionic strength samples are consistent with the observed increase in the radius of gyration and a partial unfolding of the particle.

Discussion

The results of this study indicate that 146 and 175 bp nucleosome particles show a single unfolding transition between 1.35 and 2.0 mM ionic strength. Both 146 and 175 bp particles appear to unfold at approximately the same ionic strength.

The intermediate transition (between 3 and 7 mM) observed by Schlessinger et al. (1982) for 175 bp nucleosomes and a similar transition sometimes observed for ca. 140 bp particles (Gordon et al., 1978) are not seen in this work. We propose the following explanation for this. The DNA and particle gels in Figure 1 for 146 and 175 bp nucleosomes show virtually no overlap between DNA lengths for the two kinds of particles, and there is very little evidence in the 175 bp particle of DNA significantly longer than 175 bp. In contrast, the two types of particles used by Schlessinger et al. (1982) show considerable overlap in DNA length, and the 175 bp particles contain significant amounts of much longer DNA. The intermediate state (3–7 mM) may result from a portion of the nucleosomes with very long DNA (about 200 bp) beginning to unfold at slightly higher ionic strength than the bulk of the material. Such polydispersity could lead to the observation of an average property. The expanded disk model suggested for this apparent state has characteristics which in many respects are intermediate between compact nucleosomes and an unfolded form. A similar argument was proposed by Gordon et al. (1979) to explain the intermediate state in their core nucleosomes.

The scattering curves for 146 and 175 bp nucleosomes in low ionic strength conditions are not consistent with extended cylindrical or extended helical models for unfolding. In particular, the kind of two-slope Guinier plot observed is characteristic of a particle with a large fraction of its scattering mass in a compact core region and only a small fraction in an extended conformation. Calculated values of the radius of gyration for the extended and expanded models (Schlessinger et al., 1982) are much too large, even if one assumes a compact histone core. This comparison is shown in Table IV, where the extended DNA model has been used for the 175 bp particle and the expanded DNA model for the 146 bp nucleosome.

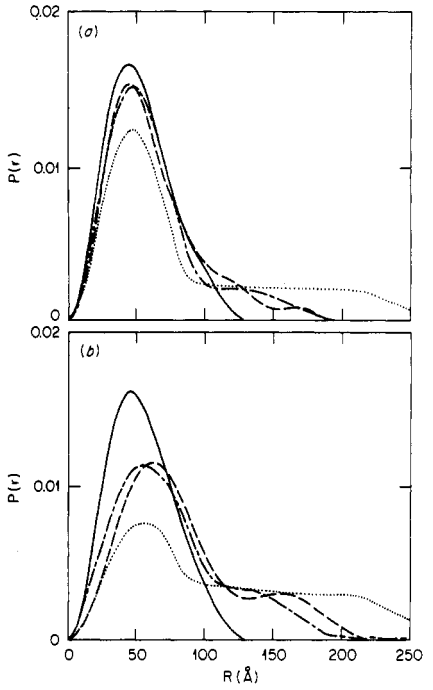

FIGURE 6: Comparison of length distribution functions for data and models for 175 bp nucleosomes. This function represents the distribution of intramolecular distances (r) and can be obtained by Fourier inversion of the scattering data. Extended nucleosomes contain long and short intramolecular distances whereas compact nucleosomes contain shorter intramolecular distances (less than 120 Å). It is possible to evaluate models for the unfolded state of nucleosomes by how well they fit the measured length distribution function. The length distribution functions for the data and the unwinding model for 146 bp nucleosomes are similar to those for the 175 bp particle, except that the longest intramolecular distances are shorter due to the shorter length of the DNA. (A) D_2O data: (—) Inversion of the measured data for 175 bp nucleosomes in D_2O at 15 mM ionic strength (well above the transition point for unfolding). The length distribution function indicates a compact nucleosome. (- - -) Inversion of the measured data for 175 bp nucleosomes in D_2O at 0.5 mM ionic strength (below the transition point for unfolding). Indications are that a portion of the nucleosome has become more extended. The effects of contrast variation indicate the extended region is DNA. (—·—) Length distribution function for our proposed unwinding model: ends unfolded and extended into the solution to leave approximately one turn of DNA wrapped around the core. This calculation is for the 175 bp nucleosome in D_2O. (···) Calculated length distribution function for the extended superhelical form of Schlessinger et al. (1982) in D_2O using the assumption that the histone core is compact (which gives the best fit for this model). The function shows a greater number of long vectors (distances) than is present from the measured neutron data. This model appears to be too extended to represent the unfolding. If the histone core is assumed to unfold in the extended superhelical model calculation, the length distribution deviates further from the measured data. (B) H_2O data: (—) Inversion of the measured H_2O data for 175 bp nucleosomes at 15 mM ionic strength (compact particle). (- - -) Inversion of the measured H_2O data for 175 bp nucleosomes at 0.5 mM ionic strength (below the unfolding transition). (—·—) Length distribution function in H_2O from the proposed unwinding model. (···) Calculated length distribution function in H_2O for the extended superhelical model of Schlessinger et al. (1982) assuming a compact histone core (best fit for this model).

The length distribution functions, $P(r)$, have been calculated from the scattering data for the high and low ionic strength situations in H_2O and D_2O (Figure 6). $P(r)$ values calculated from the extended model of Schlessinger et al. do not agree well with the observed $P(r)$ (Figure 6). The relative heights of the plateau region are very different, and the point at which $P(r)$ becomes close to 0 is also different from that obtained by using the experimental scattering data. This indicates two things: (i) the DNA is not as extended as proposed in the models of Schlessinger et al.; (ii) not all the DNA is extended,

Table IV: Predicted R_g's at Low Ionic Strength

	R_g (Å)		
	obsd value	unwinding model	extended superhelical model
175 bp			
H_2O	67	64	109
D_2O	56	53	83
			expanded model
146 bp			
H_2O		51	66
D_2O	46	44	53

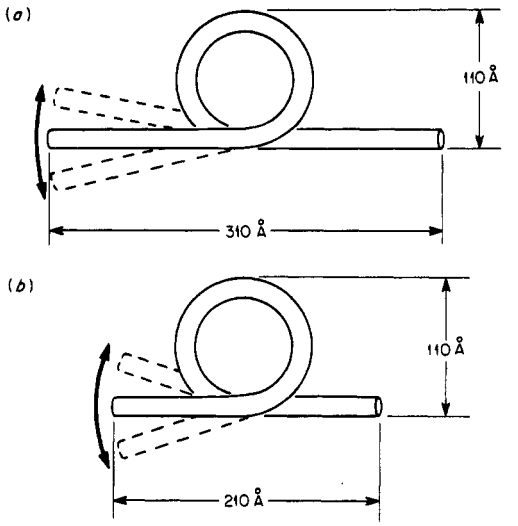

FIGURE 7: Diagram of unwinding models for 146 and 175 bp nucleosomes. DNA unwinds from the ends, leaving approximately one supercoiled turn bound to a compact core. Small changes in the histone core may take place but not an overall unfolding. The exact direction of the DNA extending into the solution is somewhat uncertain since small changes in the exit angle from the core do not significantly change the Patterson function.

implying a substantial fraction of the DNA is still wound around a compact histone core.

The model we propose for the unfolding of both 146 and 175 bp nucleosomes at low ionic strength involves retaining approximately one turn of superhelical DNA around the compact histone core, while allowing the tail regions (~30 bp for 146 bp particles and ~45 bp for 175 bp particles) to unwind from the ends and extend into the solution (see Figure 7). The observed values of the radii of gyration agree extremely well with the values calculated from this model in both H_2O and D_2O and for both 146 and 175 bp nucleosomes (Table IV). Even more striking is the close agreement between $P(r)$ calculated from this model for 146 and 175 bp nucleosomes and $P(r)$ functions obtained from the observed scattering data (Figure 6). The fact that the model agrees well with the observed data for both kinds of nucleosome particles and in both contrasts is strong evidence in its favor.

An additional test of this model is to determine the ratio of the forward scatter determined from the two different regions of the Guinier plot. This ratio should equal the ratio of the whole scattering mass to the scattering mass in the compact core. The R_g's determined from the two regions should agree with the R_g for the whole particle and the R_g of the core, respectively. The difficulty with this approach is that it is not possible to separate a particle into discrete compact and extended regions, since the change is continuous and

gradual from one region to another. However, we have done this analysis by considering the histone core and one full turn of DNA to form the compact core and the remaining DNA to be the extended shell. The calculated values of R_g for the compact core part of our model are 41.0 Å in H_2O and 37.3 Å in D_2O. In our model, the compact core has essentially the conformation of the compact 146 bp nucleosome except that there is somewhat less DNA, and as expected, the radii calculated from this model agree with experimental R_g's from compact 146 bp nucleosomes in H_2O and D_2O (37.6 and 41.9 Å, respectively). With the assumptions mentioned above, the ratio of $I(0)$'s measured has a mean of 1.21 for the 175 bp particle which compares very well to the calculated ratio of 1.19 for the scattering mass. For the 146 bp particle, the measured ratio is 1.05 compared to a calculated ratio of 1.12. Any discrepancy here is undoubtedly due to the uncertainties of the division into two discrete domains. Such uncertainties are more significant when the amount of scattering mass that is in the extended shell is smaller, as in the case of the 146 bp particle.

For this reason, we regard a test of the model $P(r)$ against the observed $P(r)$, which is equivalent to testing the model against the entire experimental scattering curve, to be a much more rigorous criterion for the agreement of a model to the experimental scattering data.

The changes in $s_{20,w}$ values from high to low ionic strength obtained here for 175 and 146 bp nucleosomes are significant but not large enough to be consistent with the extended model for 175 bp nucleosomes (Schlessinger et al., 1982) which implied a change in axial ratio from about 2:1 at higher ionic strength to over 7:1 at low ionic strength. The sedimentation data agree better with a more modest unfolding.

Many studies on nucleosome core particles have indicated that the DNA end regions are unique in character. Melting studies have demonstrated that the end regions are more labile and melt first (McGhee & Felsenfeld, 1980) and have an altered apparent helical pitch (Lutter, 1979, 1981; Bryan et al., 1979). More recent work on HMG 14 nucleosomes (Mardian et al., 1980; Sandeen et al., 1980) has demonstrated that the end regions (bp 5–25) are protected from DNase I digestion when HMG 14 is bound stoichiometrically to the nucleosome. This is consistent with the circular dichroism data of Sasi et al. (1982) on chromatin which suggest that HMG 17 directly affects the conformation of the linker region near the DNA ends and may be partially binding to this region. Studies of HMG 14–nucleosomes by neutron scattering (Uberbacher et al., 1982) and hydrodynamic methods (Harrington et al., 1982) are also consistent with changes in the conformation of the end regions, and hence the adjacent linker region.

This neutron scattering study on 146 and 175 bp nucleosomes provides further strong evidence that the DNA end regions and the adjacent linker are the most probable regions to be involved in major structural alterations that affect the functional state of the genome at the nucleosomal and polynucleosomal level. Nucleosome cross-linking data (Mirzabekov, 1980) and electron microscope image reconstructions (Klug et al., 1980) show the DNA ends to most likely be in contact with histones H2A and H2B. Apparently, the contacts between DNA and these histones are relatively few (McGhee & Felsenfeld, 1980), and the overall interaction is relatively weak. The physiological process of unfolding consistent with our data is one in which the DNA partially unwinds off the histone core by selectively breaking most contacts with H2A and H2B. In this process, HMG 14/17 might sometimes replace these lost contacts and thus stabilize the partially unwound structure.

This partial unwinding would make the linker region longer and also change the DNA exit angles from the core, implying the existence of an altered higher order structure. This does not necessarily mean a decondensing of the higher order structure. For example, McGhee et al. (1982) see no change in $s_{20,w}$ for chromatin when HMG 14/17 are bound. Nucleosomes apparently still pack into a condensed fiber, the point being that this altered fiber may be much easier to decondense when transcription is required. Other factors, such as the presence of RNA polymerase, may be necessary to decondense the fiber.

Our results are consistent with the suggestion that H2A and H2B may be removed in nucleosomes involved in transcription (Weisbrod et al., 1980), being replaced in part by HMG 14/17 proteins. In another study (Baer & Rhodes, 1983), mouse myeloma nucleosomes which bind RNA polymerase II show a deficiency in histones H2A and H2B. It is interesting that part of the suspected RNA polymerase II binding region in 146 bp nucleosomes (from bp 5–25) is the same region which apparently binds the basic portion of HMG 14/17 (Mardian et al., 1980; Uberbacher et al., 1982) and also is the region subject to unfolding at low ionic strength in this study.

In contrast to the DNA end regions, the center region of the DNA (central 85 base pairs) maintains a superhelical conformation and remains bound to the histone core [most likely with contacts to H3 and H4 (Mirzabekov, 1980; Klug et al., 1980; Nelson et al., 1982)]. A number of other studies indicate that changes in histone conformation and histone–histone interactions take place at low ionic strength. Fluorescence and sedimentation studies on 146 bp nucleosomes (Zama et al., 1978; Dieterich et al., 1979) have demonstrated that the labeled cysteine residues of H3 move somewhat apart and become more accessible to solvent. Studies of intrinsic tyrosine fluorescence on core particles (Libertini & Small, 1980, 1982) are also consistent with disruption of histone–histone interactions or changes in the histone secondary structure. Unfortunately, most of the above studies can be made consistent with a variety of models, and there appears to be little consensus as to the degree of protein core unfolding at low ionic strength.

The low ionic strength unfolding of nucleosomes as observed in this study does not lead to any measurable increase in the protein radius of gyration, and therefore, any conformational changes which may be occurring in the histone core most probably do not represent an overall unfolding of the histones. Possible conformations of the histone core which have the same R_g as in the compact particle, but in which larger changes in the shape of the core have occurred, were considered. Length distribution function analysis is not only sensitive to the R_g's of the various components of a structure but also to their shape and distribution, and this type of model will have larger numbers of longer vectors than are observed in the analysis. Furthermore, large changes in the histone core (but with the original R_g) would most likely alter the path or the entire DNA superhelix, whereas the length distribution function analysis is only consistent with perturbation of a small portion of the DNA. The changes in histone conformation and histone–histone interactions observed in fluorescence and sedimentation studies are most likely the result of "in place" or internal rearrangements of the histones which have little or no effect on the gross shape of the histone core. Furthermore, the interaction between the DNA and histones H3 and H4 apparently is to a large extent preserved. This is consistent with

digestion studies on nucleosomes (Nelson et al., 1982; Mencke & Rill, 1982) which show a large number of electrostatic interactions between the central region of the DNA and histones H3 and H4. It is not possible to determine from this study whether or not the pitch and radius of the central superhelical turn have been altered slightly by changes in histone conformation, but most likely, small changes have taken place. It is interesting to note that binding of HMG 14/17 to 146 bp nucleosomes both affects the conformation of H3 (A. E. Roberson and D. E. Olins, unpublished results) and slightly alters the conformation of the superhelical DNA (Uberbacher et al., 1982; Harrington et al., 1982), and also shows an enhanced DNase I digestion rate in portions of the center superhelical turn in poly(dA-dT) nucleosomes (Mardian et al., 1980). Active nucleosomes also have an altered H3 conformation (Weisbrod, 1982). Thus, extrapolation from this study would indicate that potentially active or even transcriptionally active nucleosomes are more likely to retain DNA contacts with conformationally altered H3 and H4 histones, while sacrificing or replacing contacts with histones H2A and H2B.

Acknowledgments

We acknowledge the strong support of W. C. Koehler, Director of the National Center for Small Angle Scattering Research, and thank him and H. R. Child for their help during the neutron measurements.

References

Baer, B. W., & Rhodes, D. (1983) *Nature (London) 301*, 482–488.

Braddock, G. W., Baldwin, J. P., & Bradbury, E. M. (1981) *Biopolymers 20*, 329–343.

Bryan, P. N., Wright, E. B., & Olins, D. E. (1979) *Nucleic Acids Res. 6*, 1449–1465.

Crothers, D. M., Dattagupta, N., Hogan, M., Klevan, L., & Lee, K. S. (1978) *Biochemistry 17*, 4525–4533.

Dieterich, A. E., Axel, R., & Cantor, C. R. (1979) *J. Mol. Biol. 129*, 587–602.

Engelman, D. M., & Moore, P. B. (1975) *Annu. Rev. Biophys. Bioeng. 4*, 219–241.

Eshaghpour, H., Dieterich, A. E., Cantor, C. R., & Crothers, D. M. (1980) *Biochemistry 19*, 1797–1805.

Gordon, V. C., Knobler, C. M., Olins, D. E., & Schumaker, V. N. (1978) *Proc. Natl. Acad. Sci. U.S.A. 75*, 660–663.

Gordon, V. C., Schumaker, V. N., Olins, D. E., Knobler, C. M., & Horwitz, J. (1979) *Nucleic Acids Res. 6*, 3845–3858.

Harrington, R. E. (1981) *Biopolymers 20*, 719–752.

Harrington, R. E., Uberbacher, E. C., & Bunick, G. J. (1982) *Nucleic Acids Res. 10*, 5695–5709.

Hewish, D. R., & Burgoyne, L. A. (1973) *Biochem. Biophys. Res. Commun. 52*, 504–510.

Hjelm, R. P., Kneale, G. G., Suau, P., Baldwin, J. P., & Bradbury, E. M. (1977) *Cell (Cambridge, Mass.) 10*, 139–151.

Jacrot, B., & Zaccai, G. (1981) *Biopolymers 20*, 2413–2426.

Klug, A., Rhodes, D., Smith, J., & Finch, J. T. (1980) *Nature (London) 287*, 509–516.

Kratky, O. (1963) *Prog. Biophys. Mol. Biol. 13*, 107–173.

Libertini, L. J., & Small, E. W. (1980) *Nucleic Acids Res. 8*, 3517–3534.

Libertini, L. J., & Small, E. W. (1982) *Biochemistry 21*, 3327–3334.

Lutter, L. C. (1978) *J. Mol. Biol. 124*, 391–420.

Lutter, L. C. (1979) *Nucleic Acids Res. 6*, 41–56.

Lutter, L. C. (1981) *Nucleic Acids Res. 9*, 4251–4265.

Mardian, J. K. W., Paton, A. E., Bunick, G. J., & Olins, D. E. (1980) *Science (Washington, D.C.) 209*, 1534–1536.

Martinson, H. G., True, R. J., & Burch, J. B. E. (1979) *Biochemistry 18*, 1082–1088.

McGhee, J. D., & Felsenfeld, G. (1980) *Nucleic Acids Res. 8*, 2751–2769.

McGhee, J. D., Rau, D. C., & Felsenfeld, G. (1982) *Nucleic Acids Res. 10*, 2007–2016.

Mencke, A. J., & Rill, R. L. (1982) *Biochemistry 21*, 4361–4370.

Mirzabekov, A. D. (1980) *Q. Rev. Biophys. 13*, 255–295.

Moore, P. B. (1980) *J. Appl. Crystallogr. 13*, 168–175.

Nelson, D. A., Mencke, A. J., Chambers, S. A., Oosterhof, D. K., & Rill, R. L. (1982) *Biochemistry 21*, 4350–4362.

Oudet, P., Spadafora, C., & Chambon, P. (1977) *Cold Spring Harbor Symp. Quant. Biol. 42*, 301–312.

Sandeen, G., Wood, W. I., & Felsenfeld, G. (1980) *Nucleic Acids Res. 8*, 3757–3778.

Sasi, R., Huvos, P. E., & Fasman, G. D. (1982) *J. Biol. Chem. 19*, 11448–11454.

Schlessinger, F. B., Dattagupta, N., & Crothers, D. M. (1982) *Biochemistry 21*, 664–669.

Sturhrmann, H. B., & Duee, E. D. (1975) *J. Appl. Crystallogr. 8*, 338–342.

Uberbacher, E. C., Mardian, J. K. W., Rossi, R. M., Olins, D. E., & Bunick, G. J. (1982) *Proc. Natl. Acad. Sci. U.S.A. 79*, 5258–5262.

Weintraub, H., & Groudine, M. (1976) *Science (Washington, D.C.) 193*, 848–856.

Weisbrod, S. T. (1982) *Nucleic Acids Res. 10*, 2017–2042.

Weisbrod, S., Groudine, M., & Weintraub, H. (1980) *Cell (Cambridge, Mass.) 19*, 289–301.

Wu, H., Dattagupta, N., Hogan, M., & Crothers, D. M. (1979) *Biochemistry 18*, 3960–3965.

Zama, M., Bryan, P. N., Harrington, R. E., Olins, A. L., & Olins, D. E. (1978) *Cold Spring Harbor Symp. Quant. Biol. 42*, 31–41.